

1 **Title**

2 High-throughput linkage mapping of Australian white cypress pine (*Callitris glaucophylla*) and map
3 transferability to related species

4

5 **Author name**

6 Shota Sakaguchi^{1,2}, Takeshi Sugino³, Yoshihiko Tsumura⁴, Motomi Ito¹, Michael D. Crisp⁵, David M. J. S.
7 Bowman⁶, Lynda D. Prior⁶, Atsushi J. Nagano^{7,8}, Mie Honjo⁷, Masaki Yasugi⁷, Hiroshi Kudo⁷, Yu Matsuki⁹,
8 Yoshihisa Suyama⁹ and Yuji Isagi³

9

10 **Author affiliation**

11 ¹ Graduate School of Arts and Sciences, The University of Tokyo, Tokyo, 153-8902 Japan; ² Research
12 Fellow of the Japan Society for the Promotion of Science; ³ Division of Forest and Biomaterials Science,
13 Graduate School of Agriculture, Kyoto University, Kyoto 6068502, Japan; ⁴ Faculty of Life and
14 Environmental Sciences, University of Tsukuba, Tsukuba, Ibaraki 3058577, Japan; ⁵ Research School of
15 Biology, The Australian National University, Canberra, ACT 2601, Australia; ⁶ School of Biological
16 Sciences, University of Tasmania, Hobart, TAS 7001, Australia; ⁷ Center for Ecological Research, Kyoto
17 University, Shiga, 5202113 Japan; ⁸ Independent Researcher in Precursory Research for Embryonic Science
18 and Technology, Japan Science and Technology Agency, ⁹ Division of Biological Resource Sciences,
19 Graduate School of Agriculture, Tohoku University, Osaki, Miyagi, 9896711 Japan

20

21 **Corresponding author**

22 Shota Sakaguchi

23 e-mail: sakaguci54@gmail.com

24

25 **Key words**

26 Ascertainment bias; *Callitris*; megagametophyte; RAD-sequencing; single tree linkage map

27 **Abstract**

28 White cypress pine (*Callitris glaucophylla*) and related species are drought-tolerant evergreen
29 conifers that occur in a wide range of bioclimatic regions in Australia.. To broaden our understanding of its
30 speciation process we applied ecological genomics to identify markers associated with environmental
31 adaptation. . We adopted a single tree linkage mapping approach combined with high-throughput RAD
32 (restriction site associated DNA) sequencing and EST-SSR genotyping to set up a baseline genetic map for
33 *C. glaucophylla*. The generated linkage map was consisted of 4,284 markers positioned on 11 linkage
34 groups, corresponding to the haploid chromosome number of *Callitris* ($2n = 22$). Map length inflation due
35 to missing observations and errors were controlled by imputing and correcting genotypes, resulting in map
36 length reduction by 76%. Spatial distribution of markers was uneven compared to random expectation with
37 significant clustering in central positions of some linkage groups, which may be associated with
38 recombination cold spots of pericentromere regions. Allelic segregation was shown to be distorted in
39 particular regions of four linkage groups, where selection may have operated on viability genes, leaving
40 allelic distortion in surrounding linked markers. We then tested RAD-SNP marker recovery in and
41 transferability of the linkage map to population genomic data collected for related *Callitris* species. Of the
42 linkage map markers, 1,257 markers (ca. 30%) were recovered in independent RAD-sequencing of *C.*
43 *glaucophylla* population samples. Genetic diversity and differentiation evaluated using mapped markers
44 reflected ascertainment bias slightly; a decrease in H_s (absolute difference of -0.018) for a related species
45 (*C. gracilis*) and an increase in F_{ST} between *C. glaucophylla* and *C. gracilis* (+0.018) were detected.
46 Although care should be taken given such biases in cross-species transfer, this study demonstrated that the
47 RAD-SNP based linkage map is essentially useful when combined with population genomic analysis of
48 this conifer lineage.

49 **Introduction**

50 Conifers are of immense ecological importance in terrestrial ecosystems (Debreczy and Racz
51 2006; Gernandt et al. 2011). They are well represented in plant communities that occur in extreme
52 environments including species that form vast coniferous forests in seasonally cold temperate/boreal
53 regions of Northern Hemisphere . The Australian genus *Callitris* (Cupressaceae) (2n=22) is the most
54 speciose and ecologically important conifer group on this predominately arid island continent (Bowman
55 and Harris 1995). While most *Callitris* species are regional endemics, the *C. columellaris* species complex
56 is unusual in terms of its continental-wide distribution extending from humid coastal to arid interior and
57 seasonally dry monsoon environments (Hill and Brodribb 1999). The complex is comprised of five
58 closely related morphospecies (*C. columellaris*, *C. intratropica*, *C. gracilis*, *C. glaucophylla*, and *C.*
59 *verrucosa*) and shows further genetic differentiation into twelve regional lineages (Sakaguchi et al. 2013).
60 Some of these species have extreme drought-tolerance () and regeneration is via continuous recruitment
61 in wetter regions or in pulses following successive wet years in arid environments (Prior et al. 2011). The
62 species has moderate tolerance to surface fires, but can be killed by high intensity grass fires ().
63 Considering its broad distribution and ecological diversification, genetic adaptation along climatic
64 gradients may have played a significant role in the speciation of this *C. columellaris* species complex.
65 Thus genomic analysis of the species complex to identify genomic regions associated with environmental
66 adaptation is expected to broaden our understanding of the diversification of this group, and more generally
67 provide insights into conifer evolution.

68 One important aspect of ecological genomics is to locate genes or genomic regions underlying
69 adaptive traits in genetic/physical maps. Unlike model species and economically important species, genome
70 sequencing is still not realistic for conifers due to their enormous genome (e.g., genome size of *Callitris*
71 species is estimated to be 8.3-11.2 pg/C in Ohri and Khoshoo 1986, which is 38-51 times larger than
72 *Arabidopsis thaliana*) (Neale et al. 2014; Nystedt et al. 2013). Thus linkage mapping has been the preferred
73 approach to mapping conifer species genomes. Early mapping studies (1990-2005) utilised markers of
74 isozyme, RAPD, ISSR, RFLP (Ritland et al. 2011), and more recently AFLP, SSR, SNP and their
75 combinations have become more popular (Chancerel et al. 2013; Kang et al. 2011; Martínez-García et al.
76 2013; Moriguchi et al. 2012; Neves et al. 2013; Pavy et al. 2012). Among these, SNPs (single nucleotide
77 polymorphisms) can be used as the most abundant genetic marker for high-resolution mapping because one
78 SNP occurs every 91 base positions on average in conifer gene sequences (González-Martínez et al. 2011).
79 A recently developed RAD-sequencing (restriction site associated DNA sequencing) is an efficient
80 technique to obtain SNP genotype data of population samples even for species with no prior genomic
81 knowledge (Baird et al. 2008; Peterson et al. 2012). This technique has been introduced to linkage mapping
82 studies and shown to be successful in generating high-density linkage maps for non-model organisms (Guo
83 et al. 2015; Kakioka et al. 2013; Talukder et al. 2014; Wu et al. 2014).

84 This study reports a high-density linkage map of white cypress pine, *Callitris glaucophylla*,

85 which was rapidly constructed by combining RAD-sequencing with single tree mapping (Tulsieram et al.
86 1992). The single tree mapping analyses haploid DNA samples, using alleles that are randomly segregated
87 from a single diploid individual. Conifers are particularly suitable for this analysis, since we can use
88 abundant open-pollinated seeds to extract haploid megagametophytes, enabling rapid linkage mapping
89 without a need for controlled crosses or mapping progenies. Our analysis focuses on three specific topics.
90 The first is on correction and imputation of SNP genotype data generated by low cost high-throughput
91 sequencing. Although high-throughput sequencing is a powerful way to obtain huge amount of sequence
92 reads, the resultant genotype data often includes many missing sequences and errors, which can hinder
93 precise estimation of map length and marker ordering (Buetow 1991; Hackett and Broadfoot 2003). To
94 compensate for such difficulties, we refined noisy RAD-SNPs data using recently developed imputation
95 and error correction methods (Ward et al. 2013; Wu et al. 2008). Secondly, we will characterise linkage
96 groups by relating our observation of heterogeneous marker density and distorted segregation along linkage
97 groups to biological processes, including variable recombination frequency and natural selection operated
98 on viability genes. Lastly, we will test marker recovery in population samples and transferability to related
99 species. A genetic map is used to illustrate genetic variation (e.g. H_s and F_{ST}) as a function of marker
100 position along linkage groups, in which information about marker position is sometimes transferred from a
101 different species/population. It matters, in these cases, how many markers are shared between species and
102 whether ascertainment bias has significant impact on population genetic statistics in a species to which map
103 information is transferred (Clark et al. 2005; Luca et al. 2011). To evaluate such uncertainties, we analysed
104 population samples of two closely related *Callitris* species using the same RAD-sequencing protocol but
105 in an independent sequencing run. Using this population data set, we will estimate marker recovery rate
106 and degree of ascertainment bias to consider the utility of our linkage map for population genomic analyses
107 of the *C. columellaris* species complex.

108 **Materials and Methods**

109 *Plant materials and DNA extraction*

110 In September 2013, seed cones were collected from a single tree of *Callitris glaucophylla*,
111 corresponding to a widespread lineage (GD in Sakaguchi et al (2013)), on the Balonne Highway,
112 Queensland, Australia (27°59'38"S, 148°21'32"E; supplementary figure 1a). The cones were kept dry in the
113 laboratory under room temperature until the seeds were discharged. After seed collection, they were soaked
114 in water overnight, and megagametophyte tissue was isolated by carefully removing the seed coat and
115 embryo under a stereo microscope. Total DNA was extracted from 88 megagametophytes and a mother tree
116 foliage sample using a hexadecyltrimethylammonium bromide (CTAB) method (Murray and Thompson
117 1980), after removing polysaccharides with isolation buffer containing 10% polyethylene glycol. DNA
118 concentration was measured using a Qubit® dsDNA BR Assay Kit (Invitrogen, Massachusetts, USA), and
119 adjusted to 10 ng/μL in all samples before genetic experiments.

120

121 *RAD-sequencing and EST-SSR genotyping*

122 In this study, a double-digest RAD library (Peterson et al. 2012) was prepared for linkage
123 mapping. Briefly, 10 ng of genomic DNA was digested with EcoRI and BglII (New England Biolabs,
124 Ipswich, Massachusetts, USA) and adapters were ligated at 37 °C overnight in 10 μL volume, which
125 contained 1 μL of 10x NEB buffer 2, 0.1μL of 100x BSA (New England Biolabs), 0.4 μL of 5 μM EcoRI
126 adapter 1 (CTCGTAGACTGCGTACC) and BglII adapter 2 (GATCGACAGTGTACTCTAGTC), 0.1 μL
127 of 100 mM ATP, and 0.5 μL of T4 DNA Ligase (Enzymatics, Beverly, Massachusetts, USA). The reaction
128 solution was then purified with AMPure®XP (Beckman Coulter, California, USA). Next, 3 μL of purified
129 DNA was used in PCR amplification in 10 μL volume, containing 1μL of each 10 μM index and PCR
130 primer 1.0 (5'-AATGATACGGCGACCACCGAGATCTACACTCTTCCCTACACGA-3'), 0.3 μL of
131 KOD-Plus-Neo enzyme and 1 μL of 10x PCR buffer (TOYOBO, Osaka, Japan), 0.6 μL of 25mM MgSO₄,
132 1 μL of 10 mM dNTP. Thermal cycling was initiated with 94 °C step for 2 min, followed by 20 cycles of
133 98 °C for 10 sec, 65 °C for 30 sec, 68 °C for 30 sec. The PCR products were pooled and purified again with
134 AMPure®XP. The purified DNA was then loaded to a 2.0 % agarose gel and fragments around 320 bp was
135 retrieved using E-Gel® SizeSelect™ (Life Technologies, Carlsbad, California, USA). After quality
136 measurement using an Agilent 2100 Bioanalyzer (Agilent Technologies, Santa Clara, California, USA), the
137 library was sequenced with 51 bp single-end reads in one lane of an Illumina HiSeq2000 (Illumina, San
138 Diego, USA) by Macrogen (Seoul, South Korea).

139 Five EST-SSRs (Ccol_rep_c1953, Ccol_rep_c10619, Ccol_rep_c10836, Ccol_rep_c12796,
140 Ccol_rep_c35787) characterized in Sakaguchi et al (2011) were used for anchoring the RAD-SNPs based
141 linkage map. The PCR reaction was carried out in a final volume of 10 μL, which contained approximately
142 5 ng of DNA, 5 μL of 2× Multiplex PCR Master Mix (Qiagen, Hilden, Germany), and 0.2 μM of each
143 primer. The PCR thermal profile involved denaturation at 95 °C for 3 min, followed by 35 cycles of 95 °C

144 for 30 sec, 53 °C for 3 min, 68 °C for 1 min and a final 7 min extension step at 68 °C. PCR products were
145 loaded onto an auto sequencer (3100 Genetic Analyser; Applied Biosystems, Carlsbad, California, USA),
146 to assess fragment lengths using GeneMapper® software (Applied Biosystems).

147

148 *Short read processing*

149 RAD-sequencing reads were filtered by Trimmomatic ver 0.32 (Bolger et al. 2014) to remove
150 the adapter and other Illumina-specific sequences and to cut low quality regions based on a quality score
151 threshold of 20, which corresponds to base call accuracy of 99% (parameter used: AVGQUAL:20,
152 LEADING:19, TRAILING:19, SLIDINGWINDOW:30:20). The cleaned reads were mapped to a RAD
153 reference for the *C. columellaris* species complex using Bowtie 2 (Langmead and Salzberg 2012) with a
154 default parameter setting in LOCAL mode. The reference, consisting of 392,320 contigs with N50 length
155 of 163 bp, was constructed by assembling RAD-sequencing reads of 10 individual trees sequenced with a
156 genome sequencer MiSeq (Illumina), using the CLC Genomics Workbench 7.5.1 (CLC bio, Aarhus,
157 Denmark) (parameter used: mismatch cost 3, insertion and deletion cost 2, length fraction 0.5, similarity
158 fraction 0.9) (see more details of the reference assembly in supplementary material 1). Mapping short reads
159 to this reference assembly was intended to allow (i) alignment of gapped-reads using Bowtie 2, (ii)
160 similarity search of longer contigs with a higher probability of blast hit, and (iii) to facilitate use of linkage
161 map information across different RAD-sequencing experiments by tracking contig IDs in the reference. A
162 similarity search of the reference contigs against an EST-library of the *C. columellaris* species complex
163 (Sakaguchi et al. 2011) was performed by a local BLAST algorithm (Altschul et al. 1990), to find the
164 contigs associated with EST sequences. The SAM files produced by Bowtie 2 were loaded to the
165 ‘ref_map.pl’ implemented in Stacks 1.08 (Catchen et al. 2011) to generate genotype data for
166 megagametophyte samples, with cross type specified as ‘DH’ (doubled haploid) with the other parameters
167 set as default.

168

169 *Linkage map construction and genotype imputation*

170 Segregation distortion of each SNP and EST-SSR marker was examined by a Chi-squared test
171 using AntMap (Iwata and Ninomiya 2006). Genome-wide distribution of allelic segregation was analysed
172 with a generalised additive model as a function of missing rate in genotype data and genomic position. A
173 Loess smoothing function was applied to the predictor of marker position on linkage groups. The GAM
174 analyses were performed using ‘gam’ library in R ver. 3.1.0 (R Development Core Team 2014).

175 Genotyping by sequencing is generally characterised by high rate of missing data and erroneous
176 SNP calling (Beissinger et al. 2013). Such data can produce apparent double or more recombination events
177 in a single sample, leading to overestimation of map length and ordering errors. In this study, the MSTmap
178 program (Wu et al. 2008) was used for marker grouping and ordering, as the algorithm is shown to
179 outperform other frequently used algorithms, particularly when the input data are noisy or incomplete (Wu

180 et al. 2008). Furthermore, Maskov ver 1.01 (Ward et al. 2013) was used to impute missing data and correct
181 erroneous genotypes, based on the marker orders estimated from initial MSTmap analysis. Samples with
182 more than 70% missing data were removed from the imputation procedure and from further mapping
183 analysis. Subsequently, the imputed genotype data were used to make the final linkage map with MSTmap,
184 with LOD criterion of 8.0 for grouping markers and Kosambi function to convert recombination value to
185 map distance (Kosambi 1943). Marker position was plotted on the linkage map using MapChart ver 2.0
186 (Voorrips 2002).

187

188 *Map coverage and marker distribution analysis*

189 Map coverage was estimated as a ratio of observed/expected genome lengths (G_o/G_e) based on
190 the method 4 described in Bishop *et al.* (1983). Spatial distribution of genetic markers on the linkage map
191 was investigated by dividing the map into 1, 5, and 10 cM intervals, and the number of markers within the
192 bins was counted, respectively. To test whether the markers were randomly distributed, expected
193 distributions of marker count under Poisson and negative binomial distributions were compared with the
194 observed data using a Chi-squared test. The Poisson distribution was generated by specifying the observed
195 mean marker density, while the observed mean and variance were used to determine the dispersion
196 parameter to calculate the expected negative binomial distribution, using ‘stats’ library in R ver. 3.1.0.

197

198 *Testing transferability of a single-tree linkage map to population genomic studies*

199 To investigate transferability of the linkage map derived from the *C. glaucophylla* to population
200 genomics of *C. columellaris* species complex, we additionally sequenced another RAD library, which
201 included population samples of *C. glaucophylla* and *C. gracilis*. The two *Callitris* species are closely related
202 and can hybridize in the areas of overlapping distributions (Sakaguchi et al. 2013) (supplementary figure
203 1a). A RAD library was prepared using the same method as described above, which included 31 samples
204 of *C. glaucophylla* and *C. gracilis* and 65 *Callitris* samples from a different research project, and these were
205 sequenced with 51 bp reads in a lane of Illumina HiSeq2000 (Illumina). After quality-based trimming using
206 Trimmomatic ver 0.32 (Bolger et al. 2014), the short reads were mapped to the *Callitris* RAD reference
207 assembly using Bowtie 2 (Langmead and Salzberg 2012) with the same parameter setting as used in the
208 linkage map analysis. The ‘ref_map.pl’ pipeline in Stacks 1.08 was used to build RAD locus, and SNP
209 genotype for each individual was exported with a minimum read depth of 8, using the ‘populations’ program
210 (Catchen et al. 2011). The exported genotype data was then processed with PLINK ver 1.07 (Purcell et al.
211 2007), filtering out markers with low allele frequency (< 0.03), missing individual rate > 0.7 , and significant
212 deviation from Hardy-Weinberg equilibrium ($P < 0.01$).

213 The R package ‘hierfstat’ (Goudet 2014) was used to calculate summary statistics of expected
214 heterozygosity (H_s) and genetic differentiation index (F_{ST}) per each marker for *C. glaucophylla* and *C.*
215 *gracilis*, respectively. To test whether the markers mapped to *C. glaucophylla*’s linkage map show biased

216 genetic variation compared to those in the overall SNP data, 1,000 subsets were randomly sampled to
217 generate distributions of mean values for each summary statistic, using the R function of 'sample' in the
218 'base' package. The distributions of mean value calculated from random subsets were compared to observed
219 means to determine statistical significance. A split tree network (Bryant and Moulton 2004) using a
220 Euclidean distance matrix was constructed using SplitsTree4 ver. 4.10 (Huson 1998) to estimate population
221 structure within the samples. In addition, STRUCTURE analysis (Pritchard et al. 2000) was performed
222 under an admixture and allele frequency correlated model (Falush et al. 2003). Using STRUCTURE ver
223 2.3, twenty independent simulations were run for $K = 2$ (i.e., assuming two genetic clusters because we
224 analysed genetic structure in two species), with 100,000 burn-in steps followed by 20,000 Markov chain
225 Monte Carlo (MCMC) steps.

226 **Results**

227 *SNP discovery by RAD-sequencing*

228 A total of 179.7 million raw single-end reads with 51 bp were obtained, yielding more than 9.1
229 gigabases. Thirteen samples with less than 0.5 million reads and one sample with an exceptionally high
230 level of heterozygosity were excluded from further analyses to reduce missing and wrongly called SNPs.
231 After quality-based filtering, the average read number for 74 included samples was 1.3 million (max. 2.5
232 million, min. 0.3 million), with 97.2 % bases having a quality score higher than 30. The filtered reads were
233 then mapped to 124,879 contigs in the RAD reference assembly, and genotypes at 7,560 markers were
234 determined at more than 55 samples. The genotype missing rate was 9.9 % on average, ranging among
235 samples from 0.7 % to 42.6 %. Graphical plotting of P values in Chi-squared tests showed apparent spatial
236 trends with genomic position (figure 2). This association was statistically significant at 9 linkage groups
237 (except for linkage groups 3 and 8), even after effects of missing rate were partialled out in GAM modelling
238 (supplementary table 1, supplementary figure 2). The markers that significantly deviated from the expected
239 segregation ratio of 1:1 ($P < 0.05$; black markers in figure 2) were excluded from the linkage map analysis.

241 *A single tree linkage map for Callitris glaucophylla*

242 On the resultant linkage map, 4,284 genetic markers including 4,279 RAD-SNPs and 5 EST-
243 SSRs were located on 11 linkage groups (figure 3, table 1, supplementary material 2), which corresponds
244 to the haploid chromosome number of *Callitris glaucophylla* (Ohri and Khoshoo 1986). A small portion of
245 the SNP markers (=67/4,279, i.e. 1.6%) showed significant hits against EST contigs (table 1). After
246 performing genotype imputation and error correction using Maskov ver 1.01, the observed map length was
247 reduced by 76.1% (from 4,324.9 cM to 1,033.5 cM; table 1), without disturbing marker orders
248 (supplementary figure 3). The imputation procedure also greatly decreased the number of unique positions
249 (from 1,325 to 585) and mean marker interval (from 1.01 cM to 0.24 cM) (table 1). When taking the
250 observed map length of 1,033.5 cM, the linkage map covered more than 99.9% of the estimated genome
251 length of *C. glaucophylla* (1034.0 cM).

252 These genetic markers showed a non-random distribution along the linkage groups. Distributions
253 of the observed marker counts were more dispersed at every bin size examined (1, 5, 10 cM), compared
254 with the expectation under a Poisson distribution (supplementary figure 4). Chi-squared tests detected
255 significant deviations at every bin size ($P < 0.01$) from both Poisson and negative binomial distributions.
256 The spatial distribution of genetic markers was heterogeneous within the linkage groups. The bins with
257 highest marker density were detected in the middle regions (LG4, 6, 8, 10 in particular) of most linkage
258 groups,, surrounded by regions with sparser markers (figure 4).

259
260 *Transferability of the linkage map to population genomics of the C. columellaris species complex*

261 Population RAD-sequencing of *C. glaucophylla* and *C. gracilis* sampled resulted in 7,472 SNP

262 markers, which met our filtering criteria. Based on these markers, split-network and STRUCTURE analysis
263 showed that the two species are clustered separately (supplementary figure 1), except for one sample
264 collected in Palinyewah, New South Wales, which was genetically intermediate (indicated by a green
265 triangle in supplementary figure 1). Therefore, in the following calculation, the potential hybrid individual
266 was excluded. When population samples were analysed for each species, the number of markers in common
267 with the *C. glaucophylla* linkage map was 1,257 (out of 6,472) for *C. glaucophylla* and 734 (of 6,476) for
268 *C. gracilis*, respectively. Of the 7,472 SNPs detected in the population analysis of the two *Callitris* species,
269 873 markers were shared in the *C. glaucophylla* linkage map. The number of SNPs mapped to each linkage
270 group was 64 on average, ranging from 45 in LG6 to 107 in LG2. H_S calculated with the mapped markers
271 (0.153) for *C. glaucophylla* was significantly larger than the values based on randomly sampled SNPs sets
272 (0.141), while the observed H_S was significantly smaller in the mapped markers for *C. gracilis* (absolute
273 difference of -0.018) (table 2). A significant difference was also detected between the genetic differentiation
274 estimates; F_{ST} between two species based on mapped markers elevated by 0.018 (table 2).

275 **Discussion**

276 In this study, a nearly saturated linkage map was constructed for *Callitris glaucophylla*, serving
277 as a first genetic map for Callitroideae, which is a Southern Hemisphere cypress lineage with great
278 ecological diversity (Enright and Hill 1995) and long evolutionary history (ca. 150 Mya; Mao et al. 2012.
279 Notably, our map building took only 3.5 months including laboratory work, sequencing and data analysis.
280 The resultant map consists of 4,284 markers over 1,033.5 cM and is one of the most comprehensive maps
281 made for any conifer. For example, some of the more extensive maps (Ritland et al. 2011) include *Pinus*:
282 2,841 markers (1,651 cM) and 2,466 markers (1,476 cM) in *P. taeda* L. (Martínez-García et al. 2013; Neves
283 et al. 2013), *Picea*: 1,216 markers (1,865 cM) in *P. mariana* (Mill.) x *P. rubens* Sarg. complex (Kang et al.
284 2011), and *Cryptomeria*: 1,262 markers (1,405 cM) in *C. japonica* (L.f.) D.Don (Moriguchi et al. 2012)].
285 Recently, genomes of two economically important Pinaceae conifers (*Picea abies* and *Pinus taeda*) have
286 been sequenced (Neale et al. 2014; Nystedt et al. 2013), thereby opening a new avenue for investigating
287 genomic evolution of these conifers. However, for most other conifer families or genera, full genome
288 sequencing is still not affordable because of their enormous genome sizes and complexity. Alternatively, as
289 demonstrated in this study, single tree mapping combined with high-throughput sequencing can be a time-
290 and cost- effective approach to build dense conifer maps for purposes of evolutionary biology, molecular
291 ecology and tree breeding.

292

293 *Influence of missing and errors in RAD-derived genotype data*

294 Despite these advantages, linkage mapping based on low-cost, high-throughput sequencing can
295 generate a substantial amount of missing data and errors, reflecting a non-uniform distribution of reads over
296 sequenced regions (Beissinger et al. 2013). In high-resolution mapping, even a low frequency of genotyping
297 error (3% and less) appears as double or multiple recombinants, and can reduce the power to order markers
298 and inflate map length (Buetow 1991; Hackett and Broadfoot 2003). In this study, initial marker ordering
299 was performed by MSTmap program, which can attain high accuracy of ordering (Kendall's $\tau > 0.989$) in
300 simulated genotype data when mapping populations whose size ($n = 100$), missing rate ($\gamma = 0.10$) and error
301 rate ($\eta = 0.10$) (Wu et al. 2008) are comparable to our raw genotype data ($n = 74$, $\gamma = 0.10$). Nevertheless,
302 the estimated map length of *C. glaucophylla* was still too large (4,324.9 cM), compared to those generally
303 reported from other conifer studies (Ritland et al. 2011). To deal with this, we subsequently performed error
304 correction and imputation based on ordered markers using Maskov ver 1.01, which decreased map length
305 greatly (by 76.1 %). The map length became closer to the value (1,405 cM) in the other Cupressaceae
306 conifer, *Cryptomeria japonica* (Moriguchi et al. 2012), which was estimated from genotype data with low
307 missing rate ($\gamma = 0.02$; Y. Moriguchi, personal communication), indicating that our map length was inflated
308 likely due to noise in genotype data. Although it was noticed that maps produced through imputation tend
309 to have fewer unique positions and thus lower resolution (Ward et al. 2013), imputation and error correction
310 is thus an indispensable step to obtain a reliable linkage map using RAD-derived genotype data.

311 As well as factors such as variation in DNA quality, library preparation, sequencing and assembly
312 errors (Pool et al. 2010), choice of restriction enzyme for efficient RAD-sequencing can have great impacts
313 on the level of genotype missing rate. Prior to this mapping study, we tested four rare-cutter enzymes (EcoRI,
314 MseI, NdeI and PstI) in pairs with BglII to screen for the most efficient enzyme species, with which
315 sufficient read depth per population sample can be obtained. After *de novo* assembling reads from 24
316 samples representing all the regional lineages of the species complex, it was shown that the number of
317 contigs containing SNPs with a missing rate less than 0.1 varied over two orders of magnitude from 494
318 (per 147,411 contigs for MseI library) to 11,617 (per 200,024 contigs for EcoRI library), which validated
319 our use of the EcoRI-BglII pair for the species. Other considerations on enzyme species would involve use
320 of hypomethylation-sensitive enzymes. It is documented that conifer genomes contain high-copy repeat
321 elements including retrotransposons, which represent 70% and 62% of genomes of *P. taeda* and *P. abies*,
322 respectively (Neale et al. 2014; Nystedt et al. 2013). Since those retrotransposon-rich regions of plant
323 genome are generally heavily methylated (Rabinowicz et al. 2005), hypomethylation-sensitive enzymes
324 can be used to establish reduced representation libraries in order to avoid highly repetitive elements
325 (Larsson et al. 2013; Pegadaraju et al. 2013). Recently, Karam et al. (2014) demonstrated a utility of RAD-
326 sequencing with a hypomethylation-sensitive enzyme to enrich gene-rich regions by sequencing *Cedrus*
327 *atlantica* Manetti, in which 17% of the contigs coding for proteins were included. This has an important
328 implication for RAD-sequencing of large-genome conifers, in which most SNPs are derived from non-
329 coding regions (98.4 % in this study). While extended linkage disequilibrium in non-coding regions of the
330 conifer genome may make it possible to perform association mapping by anonymous RAD-SNPs
331 (Moritsuka et al. 2012), there is no doubt that EST-SNPs concentrated by RAD-sequencing with
332 hypomethylation-sensitive enzymes are more useful for linking genetic polymorphisms to
333 phenotypic/environmental variation.

334

335 *Spatial heterogeneity of marker density and segregation pattern over linkage groups*

336 High-density linkage mapping studies sometimes detect strikingly marker-rich regions in linkage
337 groups (Chancerel et al. 2013; Studer et al. 2012; Talukder et al. 2014). We also found a similar pattern of
338 non-random marker distribution in *Callitris* linkage groups. Such spatially heterogeneous marker
339 distribution can be explained with respect to variable recombination rates among genomic regions (Petes
340 2001). Genome-wide surveys of recombination pattern in model plants have shown that regions of high
341 (hot spots) and low (cold spots) recombination rates are distributed along chromosomes (Gaut et al. 2007),
342 and one obvious cold spot is the heterochromatic pericentromere region where recombination is suppressed
343 (Choi et al. 2013; Wu et al. 2003). In such cold spots, recombination rarely takes place, which leads to
344 distorted genetic distances and marker clustering on the genetic map. Spatial association of a recombination
345 cold spot with a pericentromere may be the case for some linkage groups (e.g. LG4 and 6), where distinct
346 peaks of marker counts were detected at centres of linkage groups, although this cannot be confirmed

347 presently for *C. glaucophylla* without a physical map.

348 Another spatial trend found for the allelic segregation pattern was that genetic markers showing
349 significant distortions were clustered in particular regions of LG6, 7, 8, 10. Considering that the trend is
350 observed at many linked markers and consistent effects of marker position were detected even when the
351 missing rate controlled in GAM modelling, non-biological factors such as a limited number of sampled loci
352 or missing genotypes is unlikely to account for this observation. Instead, gametic or zygotic selection seems
353 to have operated on viability genes (Gillet and Gregorius 1992), leaving significant allelic distortion in
354 surrounding linked markers. Gametic selection can occur at stages from meiosis to fertilization, in which
355 the process of meiosis itself or differential survival ability among gametophytes influences marker
356 segregation, whereas random segregation is disturbed as a consequence of gametic combination
357 relationships [?] in fertilization. For allogamous forest trees, there has been evidence for substantial
358 inbreeding depression in the early stages of life cycles (Isagi et al. 2007; Naito et al. 2005), and zygotic
359 selection has been suggested in the studies that investigated allelic segregation in conifer
360 megagametophytes (Kuang et al. 1999; Siregar and Yunanto 2008). However, as the megagametophyte
361 samples used in this study are derived from open-pollinated mature seeds, it is currently difficult to exclude
362 occurrence of gametic selection or tease apart a possible interplay of gametic and zygotic selection. Future
363 studies using megagametophyte samples from different developmental stages and samples obtained from
364 selfed and outcrossed seeds would be meaningful for testing these hypotheses.

365

366 *SNP recovery in independent population sequencings and map transferability*

367 Since genetic diversity and differentiation levels greatly vary among genomic regions in conifers
368 (Eckert et al. 2010; Li et al. 2010; Tsumura et al. 2007; Tsumura et al. 2014), any markers linked to genetic
369 maps are important for obtaining a more detailed picture of genomic evolution. In this study, ca. 30% of
370 SNPs (1,257 markers) in the *C. glaucophylla* linkage map were recovered in independent population RAD-
371 sequencing of the same species. This finding indicates that these markers with known map positions could
372 improve our understanding of the evolution of the *C. columellaris* species complex, by extending a
373 population genetic analysis that used only 30 EST-SSR markers (Sakaguchi et al. 2013).

374 When applying map information to population analyses, however, we should be aware that the
375 mapped markers may suffer from ascertainment bias. Ascertainment bias arises because usually only a
376 small number of samples are used to identify markers, with which genetic polymorphism is maximized. It
377 follows that the selected markers do not represent the polymorphism preserved in whole populations, and
378 estimated the allele frequency spectrum becomes skewed compared to one obtained from genome
379 sequencing (Albrechtsen et al. 2010). In this study, we found that genetic diversity of *C. gracilis* and
380 differentiation between two *Callitris* species was slightly, but significant statistically, , under- or over-
381 estimated at the mapped SNPs in comparison to the randomly sampled. The detected effects on summary
382 statistics were within expectation as the markers were screened from only a single tree, and showed a pattern

383 consistent with that reported in human studies (Clark et al. 2005; Luca et al. 2011). Another source of bias
384 in summary statistics may have been introduced from the RAD-sequencing technique itself. Because RAD-
385 sequencing uses restriction enzymes for preparing a reduced representation library, a polymorphism in a
386 restriction site can result in allele drop-out where a heterozygous sample appears as a homozygote due to a
387 null allele (Arnold et al. 2013; Gautier et al. 2013). Hence, it can also lead to biased estimates of population
388 summary statistics if allelic drop-out tends to occur at higher probability in populations genetically diverged
389 from the population in which the linkage map was constructed.

390 Increasing the ascertainment sample size can reduce ascertainment bias (Albrechtsen et al. 2010).
391 In the case of linkage mapping, it would be effective to construct linkage maps from multiple
392 populations/species in *C. columellaris* species complex and join them to make a consensus map with
393 common markers segregating in two or more mapping populations. Such a map would include SNP markers
394 that can capture genetic polymorphism with less ascertainment bias when applied to whole population
395 analysis. It is also desirable to include species in linkage mapping that show the highest levels of genetic
396 divergence, as the number of SNPs shared between congenic species are shown to be inversely related to
397 phylogenetic distances (Pavy et al. 2013). Although we need to deal carefully with ascertainment bias, the
398 RAD-SNPs based linkage map is essentially useful in combined with population genomic analyses of *C.*
399 *columellaris* species complex. Promising applications of the map information will include detection of
400 linkage disequilibrium arising from genetic admixture (Falush et al. 2003) and identification of genomic
401 regions that are associated with particular adaptive traits and show significant divergence due to natural
402 selection (Andrew and Rieseberg 2013; Chutimanitsakun et al. 2011; Slavov et al. 2014). These factors
403 should have played significant roles in speciation and environmental adaptation of the conifer lineage.

404 **Acknowledgements**

405 We are grateful to NSW State Forests, NSW Department of Environment and Climate Change,
406 Queensland Department of Environment and Resource Management, SA Department of Environment and
407 Heritage, Victorian Department of Sustainability and Environment, the Australian Wildlife Conservancy
408 and many private landholders for help with site selection and permission to sample on their land. We thank
409 N. Nakahama and Y. Unno for their assists in genotyping EST-SSRs and a preliminary analysis, M.
410 Yamasaki for his insightful discussions on statistical analysis, and Y. Moriguchi for kindly providing
411 unpublished data. Funding was provided by Japan Society for the Promotion of Science Grant-in-Aid for
412 JSPS Fellows (13J06059), Grant-in-Aid for Scientific Research (JSPS KAKENHI 24248028 and
413 26850098), and the Environment Research and Technology Development Fund of the Ministry of the
414 Environment (4-1403).

415 **Table 1**

416 Statistics for of the lineage map of *Callitris glaucophylla*.

417

Linkage group	No. of Markers			Length (cM)		No. of unique position		Mean marker interval (cM)	Mean interval of unique position (cM)
	total	SNPs (EST SNPs)	EST-SSR	without imputation	with imputation	without imputation	with imputation		
LG1	486	486 (4)	0	400.6	109.2	127	59	0.22	1.85
LG2	456	456 (10)	0	425.2	104.3	132	63	0.23	1.66
LG3	468	467 (6)	1	501.4	98.6	160	59	0.21	1.67
LG4	359	358 (1)	1	483.1	95.7	128	46	0.27	2.08
LG5	358	358 (6)	0	424.2	95.6	125	56	0.27	1.71
LG6	351	351 (7)	0	395.5	94.3	117	53	0.27	1.78
LG7	358	358 (8)	0	376.3	94.2	113	49	0.26	1.92
LG8	352	352 (8)	0	309.6	91.5	101	50	0.26	1.83
LG9	344	343 (8)	1	273.0	84.6	86	47	0.25	1.80
LG10	361	361 (3)	0	345.8	84.3	113	53	0.23	1.59
LG11	391	389 (6)	2	390.3	81.2	123	50	0.21	1.62
	4,284	4,279 (67)	5	4,324.9	1,033.5	1,325	585	0.24	1.77

418

419 **Table 2**

420 Comparison of summary statistics of genetic diversity between the mapped SNP markers to *Callitris*
 421 *glaucophylla* linkage map and the randomly sampled SNP markers.

422

Summary statistics	Obs. mean of the mapped markers	Mean (99% points) of the sampled markers	Absolute difference in mean values	<i>P</i> value
<i>Hs</i> (<i>C. glaucophylla</i>)	0.153	0.128 (0.117, 0.139)	+0.025	< 0.01
<i>Hs</i> (<i>C. gracilis</i>)	0.098	0.116 (0.105, 0.127)	-0.018	< 0.01
<i>F_{ST}</i>	0.064	0.046 (0.037, 0.055)	+0.018	< 0.01

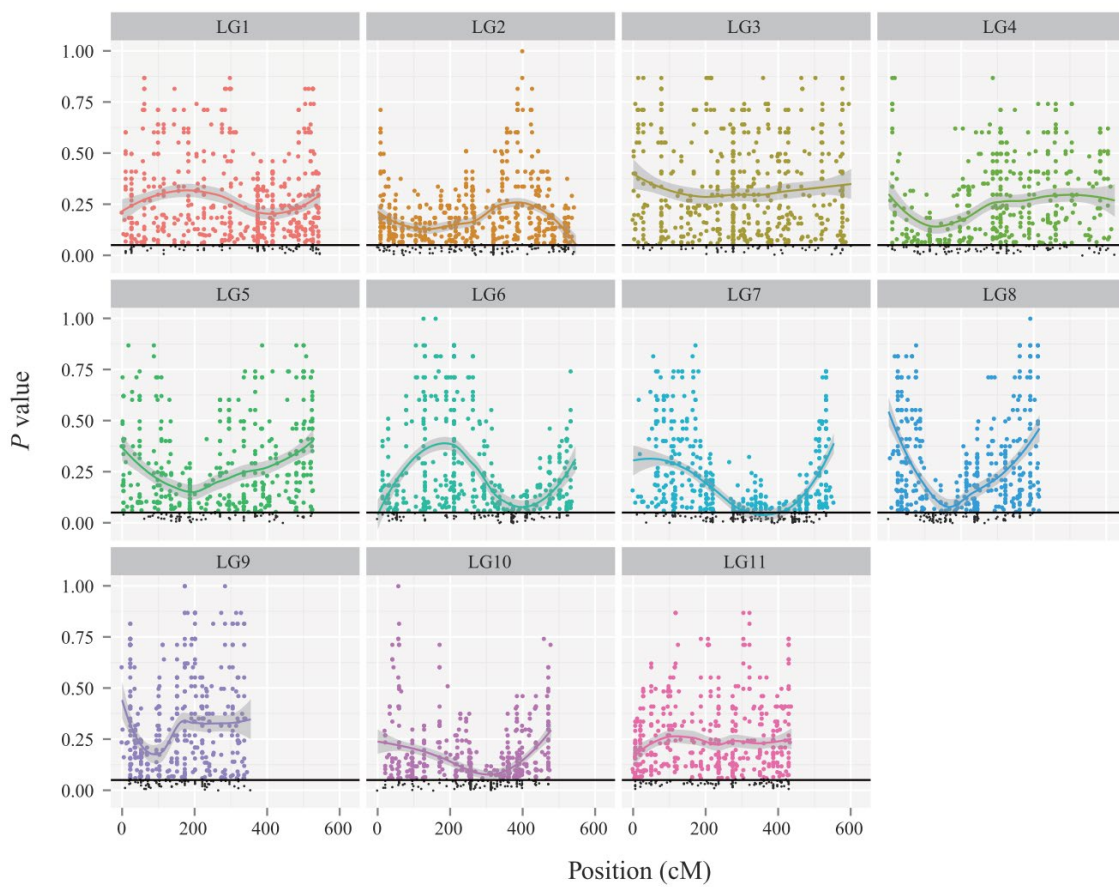
423

424 **Figure 1**

425 Genome-wide distribution of marker segregation pattern, represented by P value in Chi-squared tests
426 against marker position on the eleven linkage groups. Smoothing curves using the loess method with 95%
427 CI are also shown. The dropped markers showing significant deviation from the expected 1:1 segregation
428 ratio ($P < 0.05$) are indicated by black points.

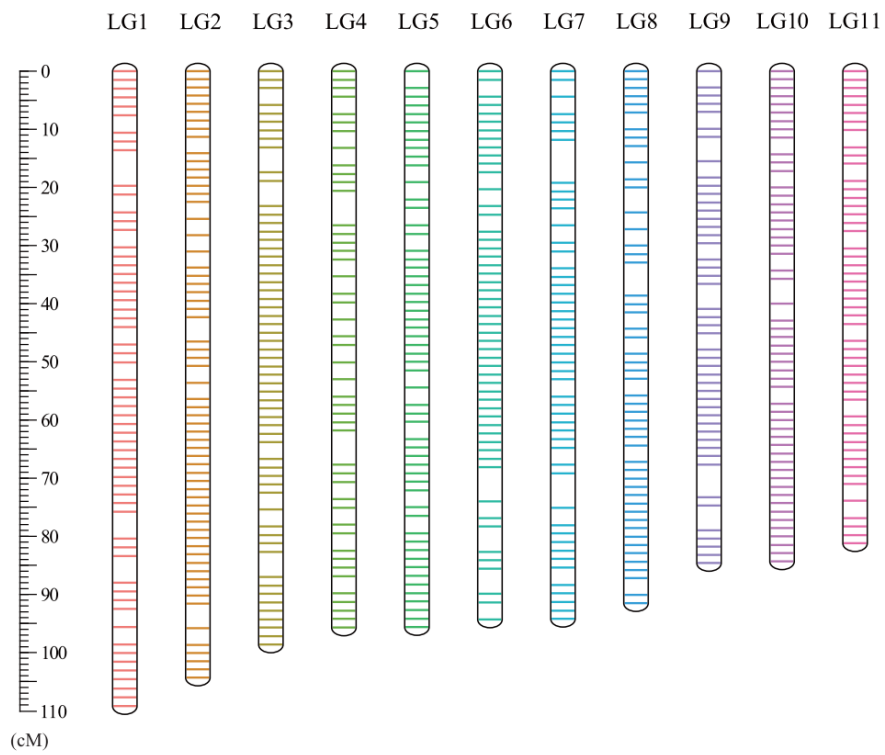
429

430



431 **Figure 2**

432 Linkage map for *Callitris glaucophylla* composed of 4,284 genetic markers of 4,279 SNPs (including 67
433 EST-SNPs) and 5 EST-SSRs. Unique positions estimated after data imputation procedure are shown on the
434 eleven linkage groups, which correspond to the haploid set of 11 chromosomes.
435

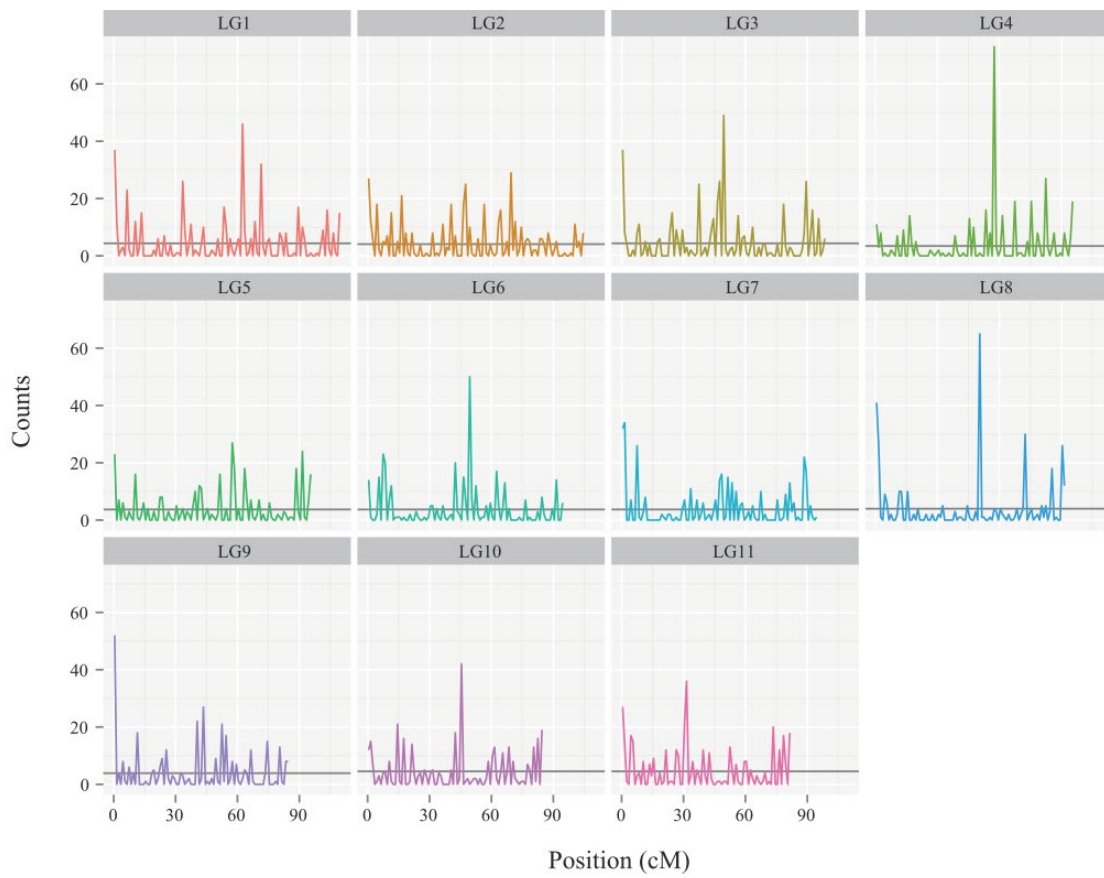


436 **Figure 3**

437 Spatial distribution of marker density as evaluated with a bin width of 1 cM. Marker counts are plotted
438 against marker positions (mid position of each bin). Horizontal lines shows mean marker counts across
439 linkage groups.

440

441



442 **Supplementary table 1**

443 Results of GAM analysis of genetic marker segregation for each linkage group, as a function of missing
 444 rate in genotype data and map position.

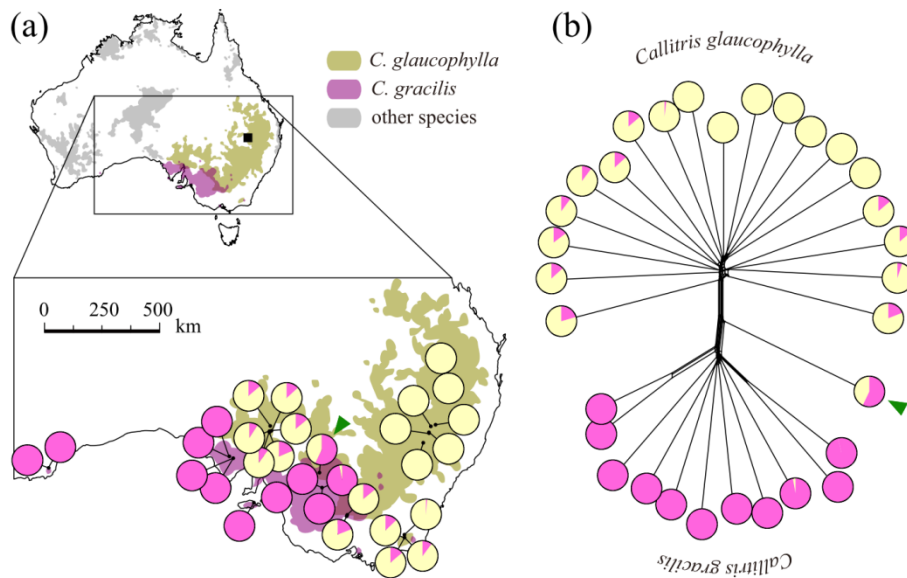
445

Linkage group	AIC	Missing rate		Map position	
		<i>F</i> value	<i>P</i> value	<i>F</i> value	<i>P</i> value
LG1	-925.3	1,347.6	< 0.01	19.0	< 0.01
LG2	-929.4	475.6	< 0.01	15.1	< 0.01
LG3	-1,018.3	2,592.1	< 0.01	0.2	0.61
LG4	-717.4	944.4	< 0.01	78.8	< 0.01
LG5	-785.1	1,446.8	< 0.01	30.5	< 0.01
LG6	-617.1	763.2	< 0.01	42.7	< 0.01
LG7	-756.4	524.8	< 0.01	79.4	< 0.01
LG8	-652.6	841.1	< 0.01	0.29	0.58
LG9	-542	1,037.6	< 0.01	26.9	< 0.01
LG10	-833.5	354.6	< 0.01	4.2	0.04
LG11	-860.8	1,115.5	< 0.01	5.6	0.02

446 **Supplementary figure 1**

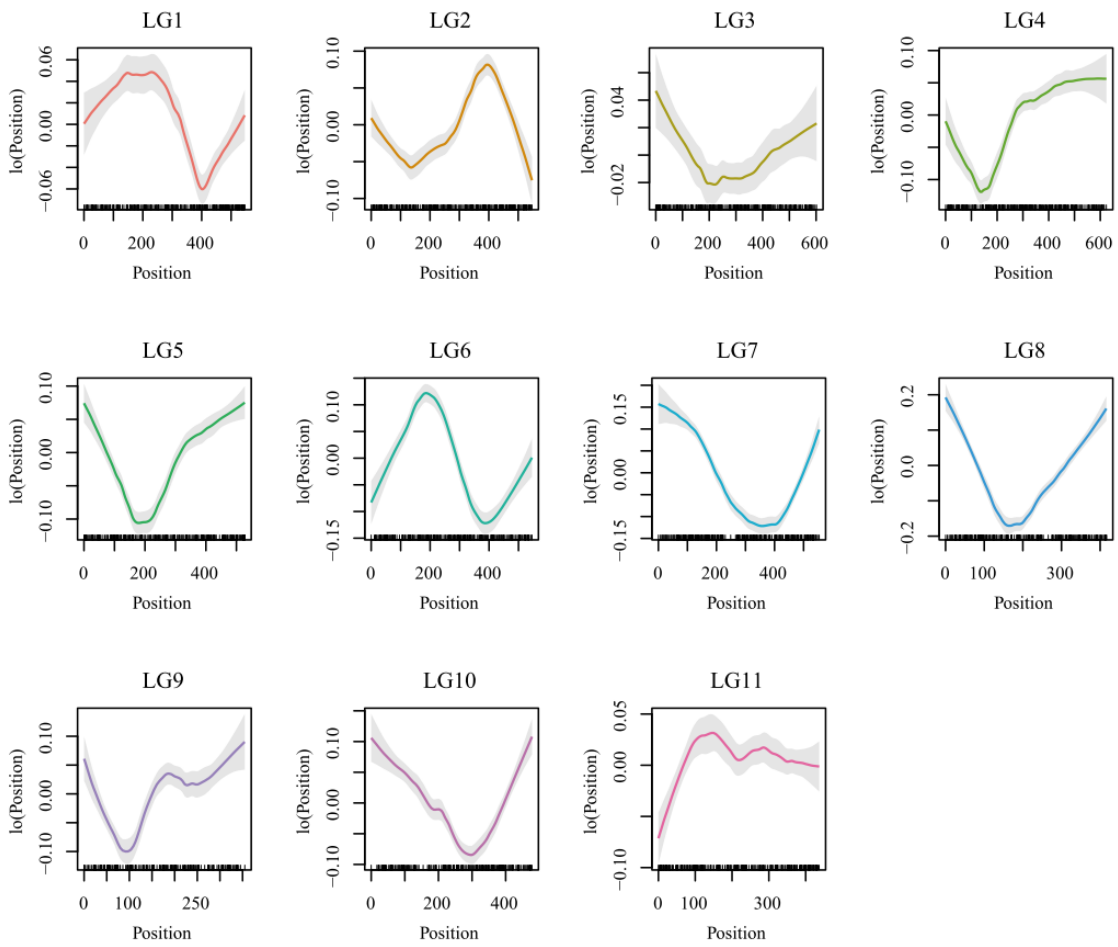
447 (a) Distribution of *Callitris columellaris* species complex. Ranges for *C. glaucophylla* (GD lineage) and *C.*
448 *gracilis* are colored by ochre and pink, respectively. The locality where the seed samples for linkage map
449 construction were collected is indicated by a black square on the smaller map. Superimposed are pie charts
450 illustrating the two genetic clusters, corresponding to the two species, which were detected by
451 STRUCTURE analysis. (b) A split network for 31 individuals of *C. glaucophylla* and *C. gracilis* analysed
452 in this study. Genetic membership estimated from STRUCTURE analysis is placed on the tips. A genetically
453 intermediate individual is indicated by a green triangle.

454



455 **Supplementary figure 2**

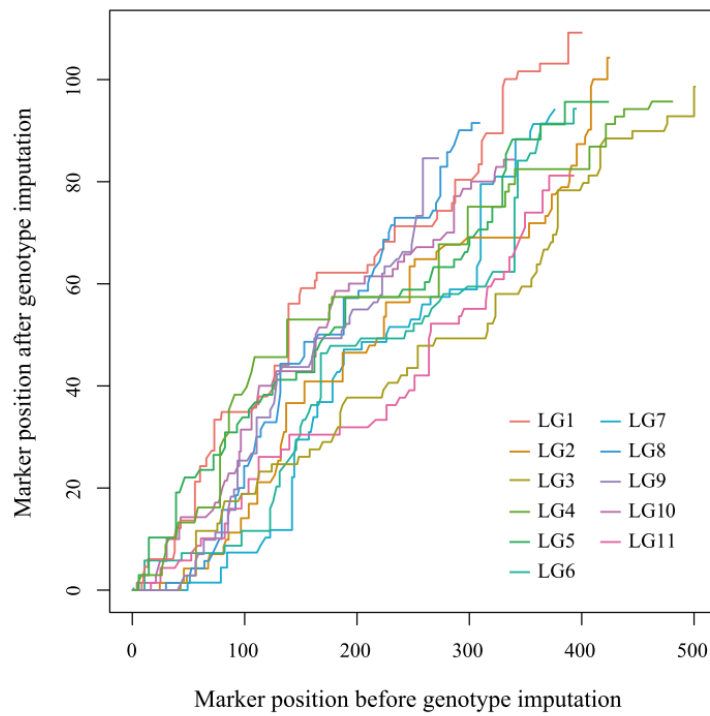
456 Graphical results of GAM analysis of genetic marker segregation. Partial effects of genomic position are
457 shown for each linkage group, expressed as fitted loess functions with 95% boot-strapped confidence
458 intervals (gray in color). Ticks in the x-axis represent the location of observations along the predictor.



459 **Supplementary figure 3**

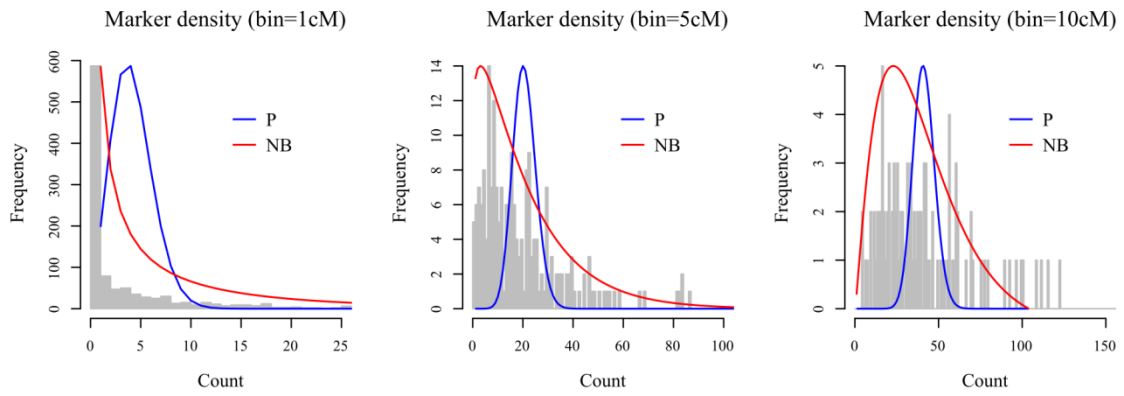
460 Relationship between marker positions estimated from genotype data sets with and without imputation and
461 error correction procedures.

462



463 **Supplementary figure 4**

464 Distribution of genetic marker density calculated based on different bin widths (1, 5, 10 cM). Expected
465 probability curves are estimated using a Poisson distribution (blue) and a negative binomial distribution
466 (red).



467 **References**

468

- 469 Albrechtsen A, Nielsen FC, Nielsen R (2010) Ascertainment biases in SNP chips affect measures of
470 population divergence Mol Biol Evol:msq148
- 471 Altschul SF, Gish W, Miller W, Myers EW, Lipman DJ (1990) Basic Local Alignment Search Tool J Mol
472 Biol 215:403-410
- 473 Andrew RL, Rieseberg LH (2013) Divergence is focused on few genomic regions early in speciation:
474 incipient speciation of sunflower ecotypes Evolution 67:2468-2482
- 475 Arnold B, Corbett - Detig R, Hartl D, Bomblies K (2013) RADseq underestimates diversity and introduces
476 genealogical biases due to nonrandom haplotype sampling Mol Ecol 22:3179-3190
- 477 Baird NA et al. (2008) Rapid SNP discovery and genetic mapping using sequenced RAD markers PLoS
478 One 3:e3376
- 479 Beissinger TM et al. (2013) Marker density and read depth for genotyping populations using genotyping-
480 by-sequencing Genetics 193:1073-1081
- 481 Bishop D, Cannings C, Skolnick M, Williamson J, Weir B (1983) The number of polymorphic DNA clones
482 required to map the human genome. In: Statical analysis of DNA sequence data. Marcel-Dekker,
483 New York, pp 181-200
- 484 Bolger AM, Lohse M, Usadel B (2014) Trimmomatic: a flexible trimmer for Illumina sequence data
485 Bioinformatics 30:2114-2120 doi:10.1093/bioinformatics/btu170
- 486 Bowman D, Harris S (1995) Conifers of Australia's dry forests and open woodlands. In: Enright N, Hill R
487 (eds) Ecology of Southern Conifers. University of Melbourne, Melbourne, pp 252-270
- 488 Bryant D, Moulton V (2004) Neighbor-Net: An agglomerative method for the construction of phylogenetic
489 networks Mol Biol Evol 21:255-265
- 490 Buetow KH (1991) Influence of aberrant observations on high-resolution linkage analysis outcomes Am J
491 Hum Genet 49:985
- 492 Catchen JM, Amores A, Hohenlohe P, Cresko W, Postlethwait JH (2011) Stacks: Building and Genotyping
493 Loci De Novo From Short-Read Sequences G3-Genes Genomes Genetics 1:171-182
494 doi:10.1534/g3.111.000240
- 495 Chancerel E et al. (2013) High-density linkage mapping in a pine tree reveals a genomic region associated
496 with inbreeding depression and provides clues to the extent and distribution of meiotic
497 recombination BMC Biology 11:50
- 498 Choi K et al. (2013) *Arabidopsis* meiotic crossover hot spots overlap with H2A. Z nucleosomes at gene
499 promoters Nature genetics 45:1327-1336
- 500 Chutimanitsakun Y et al. (2011) Construction and application for QTL analysis of a Restriction Site
501 Associated DNA (RAD) linkage map in barley BMC Genomics 12:4

502 Clark AG, Hubisz MJ, Bustamante CD, Williamson SH, Nielsen R (2005) Ascertainment bias in studies of
503 human genome-wide polymorphism *Genome Res* 15:1496-1502

504 Debreczy Z, Racz I (2006) *Conifers around the world vol II*. DendroPress Limited, Budapest

505 Eckert AJ, van Heerwaarden J, Wegrzyn JL, Nelson CD, Ross-Ibarra J, Gonzalez-Martinez SC, Neale DB
506 (2010) Patterns of Population Structure and Environmental Associations to Aridity Across the
507 Range of Loblolly Pine (*Pinus taeda* L., Pinaceae) *Genetics* 185:969-982
508 doi:10.1534/genetics.110.115543

509 Enright N, Hill R (1995) *Ecology of Southern Conifers*. University of Melbourne, Melbourne

510 Falush D, Stephens M, Pritchard JK (2003) Inference of population structure using multilocus genotype
511 data: linked loci and correlated allele frequencies *Genetics* 164:1567-1587

512 Gaut BS, Wright SI, Rizzon C, Dvorak J, Anderson LK (2007) Recombination: an underappreciated factor
513 in the evolution of plant genomes *Nat Rev Genet* 8:77-84

514 Gautier M et al. (2013) The effect of RAD allele dropout on the estimation of genetic variation within and
515 between populations *Mol Ecol* 22:3165-3178

516 Gernandt D, Willyard A, Syring JV, Liston A (2011) The Conifers (Pinophyta). In: Plomion C, Bousquet J,
517 Kole C (eds) *Genetics, Genomics and Breeding of Conifers*. CRC Press, pp 1-39

518 Gillet E, Gregorius HR (1992) What can be inferred from open-pollination progenies about the source of
519 observed segregation distortion? - a case study in *Castanea sativa* Mill. *Silvae Genetica* 41:82-87

520 González-Martínez S et al. (2011) Patterns of nucleotide diversity and association mapping. In: *Genetics,*
521 *genomics and breeding of conifers*. pp 239-275

522 Gouded J (2014) hierfstat: Estimation and tests of hierarchical F-statistics. R-package.

523 Guo F et al. (2015) Construction of a SNP-based high-density genetic map for pummelo using RAD
524 sequencing *Tree Genetics & Genomes* 11:1-11 doi:10.1007/s11295-014-0831-0

525 Hackett C, Broadfoot L (2003) Effects of genotyping errors, missing values and segregation distortion in
526 molecular marker data on the construction of linkage maps *Heredity* 90:33-38

527 Hill RS, Brodribb TJ (1999) Turner Review No. 2 - Southern conifers in time and space *Aust J Bot* 47:639-
528 696

529 Huson DH (1998) SplitsTree: analyzing and visualizing evolutionary data *Bioinformatics* 14:68-73

530 Isagi Y, Saito D, Kawaguchi H, Tateno R, Watanabe S (2007) Effective pollen dispersal is enhanced by the
531 genetic structure of an *Aesculus turbinata* population *J Ecol* 95:983-990 doi:10.1111/j.1365-
532 2745.2007.01272.x

533 Iwata H, Ninomiya S (2006) AntMap: Constructing genetic linkage maps using an ant colony optimization
534 algorithm *Breed Sci* 56:371-377 doi:10.1270/jsbbs.56.371

535 Kakioka R, Kokita T, Kumada H, Watanabe K, Okuda N (2013) A RAD-based linkage map and comparative
536 genomics in the gudgeons (genus *Gnathopogon*, Cyprinidae) *Bmc Genomics* 14:32

537 Kang B-Y, Major JE, Rajora OP (2011) A high-density genetic linkage map of a black spruce (*Picea*

538 *mariana*)× red spruce (*Picea rubens*) interspecific hybrid Genome 54:128-143

539 Karam MJ, Lefèvre F, Dagher - Kharrat MB, Pinosio S, Vendramin G (2014) Genomic exploration and
540 molecular marker development in a large and complex conifer genome using RADseq and
541 mRNAseq Mol Ecol Resour

542 Kosambi DD (1943) The estimation of map distances from recombination values AnnEug 12:172-175

543 Kuang H, Richardson T, Carson S, Wilcox P, Bongarten B (1999) Genetic analysis of inbreeding depression
544 in plus tree 850.55 of *Pinus radiata* D. Don. I. Genetic map with distorted markers Theor Appl
545 Genet 98:697-703

546 Langmead B, Salzberg SL (2012) Fast gapped-read alignment with Bowtie 2 Nature Methods 9:357-U354
547 doi:10.1038/nmeth.1923

548 Larsson H, De Paoli E, Morgante M, Lascoux M, Gyllenstrand N (2013) The Hypomethylated Partial
549 Restriction (HMPCR) method reduces the repetitive content of genomic libraries in Norway spruce
550 (*Picea abies*) Tree Genetics & Genomes 9:601-612

551 Li S, Chen Y, Gao H, Yin T (2010) Potential chromosomal introgression barriers revealed by linkage
552 analysis in a hybrid of *Pinus massoniana* and *P. hwangshanensis* BMC Plant Biology 10 doi:37
553 10.1186/1471-2229-10-37

554 Luca F, Hudson RR, Witonsky DB, Di Rienzo A (2011) A reduced representation approach to population
555 genetic analyses and applications to human evolution Genome Res 21:1087-1098

556 Mao KS et al. (2012) Distribution of living Cupressaceae reflects the breakup of Pangea Proc Natl Acad
557 Sci U S A 109:7793-7798 doi:10.1073/pnas.1114319109

558 Martínez-García PJ, Stevens KA, Wegrzyn JL, Liechty J, Crepeau M, Langley CH, Neale DB (2013)
559 Combination of multipoint maximum likelihood (MML) and regression mapping algorithms to
560 construct a high-density genetic linkage map for loblolly pine (*Pinus taeda* L.) Tree Genetics &
561 Genomes 9:1529-1535

562 Moriguchi Y et al. (2012) The construction of a high-density linkage map for identifying SNP markers that
563 are tightly linked to a nuclear-recessive major gene for male sterility in *Cryptomeria japonica* D.
564 Don BMC Genomics 13:95

565 Moritsuka E, Hisataka Y, Tamura M, Uchiyama K, Watanabe A, Tsumura Y, Tachida H (2012) Extended
566 linkage disequilibrium in noncoding regions in a conifer, *Cryptomeria japonica* Genetics
567 190:1145-1148

568 Murray MG, Thompson WF (1980) Rapid isolation of high molecular weight plant DNA Nucleic Acids
569 Res 8:4321-4325

570 Naito Y et al. (2005) Selfing and inbreeding depression in seeds and seedlings of *Neobalanocarpus heimii*
571 (Dipterocarpaceae) J Plant Res 118:423-430

572 Neale DB et al. (2014) Decoding the massive genome of loblolly pine using haploid DNA and novel
573 assembly strategies Genome biology 15:R59

574 Neves LG, Davis JM, Barbazuk WB, Kirst M (2013) A high-density gene map of loblolly pine (*Pinus taeda*
575 L.) based on exome sequence capture genotyping G3: Genes| Genomes| Genetics:g3. 113.008714
576 Nystedt B et al. (2013) The Norway spruce genome sequence and conifer genome evolution Nature
577 497:579-584 doi:10.1038/nature12211
578
579 Ohri D, Khoshoo T (1986) Genome size in gymnosperms Plant Syst Evol 153:119-132
580 Pavy N et al. (2013) Development of high - density SNP genotyping arrays for white spruce (*Picea glauca*)
581 and transferability to subtropical and nordic congeners Mol Ecol Resour 13:324-336
582 Pavy N, Pelgas B, Laroche J, Rigault P, Isabel N, Bousquet J (2012) A spruce gene map infers ancient plant
583 genome reshuffling and subsequent slow evolution in the gymnosperm lineage leading to extant
584 conifers BMC Biol 10:84
585 Pegadaraju V, Nipper R, Hulke B, Qi L, Schultz Q (2013) De novo sequencing of sunflower genome for
586 SNP discovery using RAD (Restriction site Associated DNA) approach BMC Genomics 14:556
587 Peterson BK, Weber JN, Kay EH, Fisher HS, Hoekstra HE (2012) Double Digest RADseq: An Inexpensive
588 Method for *De Novo* SNP Discovery and Genotyping in Model and Non-Model Species PLoS One
589 7:e37135 doi:10.1371/journal.pone.0037135
590 Petes TD (2001) Meiotic recombination hot spots and cold spots Nat Rev Genet 2:360-369
591 Pool JE, Hellmann I, Jensen JD, Nielsen R (2010) Population genetic inference from genomic sequence
592 variation Genome Res 20:291-300
593 Prior LD, McCaw WL, Grierson PF, Murphy BP, Bowman DMJS (2011) Population structures of the
594 widespread Australian conifer *Callitris columellaris* are a bio-indicator of continental
595 environmental change For Ecol Manage 262:252-262 doi:10.1016/j.foreco.2011.03.030
596 Pritchard JK, Stephens M, Donnelly P (2000) Inference of population structure using multilocus genotype
597 data Genetics 155:945-959
598 Purcell S et al. (2007) PLINK: A tool set for whole-genome association and population-based linkage
599 analyses Am J Hum Genet 81:559-575 doi:10.1086/519795
600 R Development Core Team (2014) R version 3.1.0: A language and environment for statistical computing
601 Rabinowicz PD et al. (2005) Differential methylation of genes and repeats in land plants Genome Res
602 15:1431-1440
603 Ritland K, Krutovsky KV, Tsumura Y, Pelgas B, Isabel N, Bousquet J (2011) Genetic mapping in conifers.
604 In: Genetics, genomics and breeding of conifers. CRC Press, pp 196-238
605 Sakaguchi S, Bowman DMJS, Prior LD, Crisp MD, Linde CC, Tsumura Y, Isagi Y (2013) Climate, not
606 Aboriginal landscape burning, controlled the historical demography and distribution of fire-
607 sensitive conifer populations across Australia Proceedings of the Royal Society B: Biological
608 Sciences 280 doi:10.1098/rspb.2013.2182
609 Sakaguchi S et al. (2011) Isolation and characterization of 52 polymorphic EST-SSR markers for *Callitris*

610 *columellaris* (Cupressaceae) Am J Bot 98:E363-E368 doi:10.3732/ajb.1100276

611 Siregar IZ, Yunanto T (2008) Inference on the Possible Causes of Segregation Distortion from Open
612 Pollination Progenies of Merkus Pine (*Pinus merkusii*) HAYATI Journal of Biosciences 15:173

613 Slavov GT et al. (2014) Genome-wide association studies and prediction of 17 traits related to phenology,
614 biomass and cell wall composition in the energy grass *Miscanthus sinensis* New Phytol 201:1227-
615 1239 doi:10.1111/nph.12621

616 Studer B et al. (2012) A transcriptome map of perennial ryegrass (*Lolium perenne* L.) Bmc Genomics
617 13:140

618 Talukder ZI, Gong L, Hulke BS, Pegadaraju V, Song Q, Schultz Q, Qi L (2014) A high-density SNP map
619 of sunflower derived from RAD-sequencing facilitating fine-mapping of the rust resistance gene
620 R12 PLoS One 9:e98628

621 Tsumura Y, Kado T, Takahashi T, Tani N, Ujino-Ihara T, Iwata H (2007) Genome scan to detect genetic
622 structure and adaptive genes of natural populations of *Cryptomeria japonica* Genetics 176:2393-
623 2403

624 Tsumura Y, Uchiyama K, Moriguchi Y, Kimura MK, Ueno S, Ujino-Ihara T (2014) Genetic Differentiation
625 and Evolutionary Adaptation in *Cryptomeria japonica* G3: Genes| Genomes| Genetics 4:2389-
626 2402

627 Tulsieram LK, Glaubitz JC, Kiss G, Carlson JE (1992) Single tree genetic linkage mapping in conifers
628 using haploid DNA from megagametophytes Nature Biotechnology 10:686-690

629 Voorrips RE (2002) MapChart: Software for the graphical presentation of linkage maps and QTLs J Hered
630 93:77-78 doi:10.1093/jhered/93.1.77

631 Ward JA et al. (2013) Saturated linkage map construction in *Rubus idaeus* using genotyping by sequencing
632 and genome-independent imputation BMC Genomics 14 doi:2
633 10.1186/1471-2164-14-2

634 Wu J et al. (2014) High-density genetic linkage map construction and identification of fruit-related QTLs
635 in pear using SNP and SSR markers Journal of Experimental Botany doi:10.1093/jxb/eru311

636 Wu J et al. (2003) Physical maps and recombination frequency of six rice chromosomes The Plant Journal
637 36:720-730

638 Wu Y, Bhat PR, Close TJ, Lonardi S (2008) Efficient and accurate construction of genetic linkage maps
639 from the minimum spanning tree of a graph PLoS genetics 4:e1000212

640

641

Construction of RAD reference assembly of *Callitris columellaris* species complex

DNA samples of 10 individuals (representing 9 regions in Australia and 5 morphospecies of the species complex) were digested by with EcoRI and BglII, and prepared for RAD-sequencing using the same protocol as taken in the linkage mapping analysis. The sample information of samples are summarised as follows.

Sample No.	Species	Region	Population	Latitude	Longitude	Restriction enzymes	No. reads used for <i>de novo</i> assembly
1	<i>C. intratropica</i>	Kimberley	CintK6	-16° 56'	126° 13'	EcoRI – BglII	993,398
2	<i>C. intratropica</i>	The Top End	CintTE5	-13° 13'	132° 39'	EcoRI – BglII	614,007
4	<i>C. intratropica</i>	Cape York Peninsula	CintNQ1	-17° 08'	145° 38'	EcoRI – BglII	824,954
5	<i>C. columellaris</i>	Central Eastern Coast	CcolQC	-28° 48'	153° 22'	EcoRI – BglII	1,679,270
7	<i>C. gracilis</i>	Murray Basin	CgrHKA	-35° 24'	142° 23'	EcoRI – BglII	1,340,960
10	<i>C. glaucophylla</i>	Great Dividing Range	CglSQ3	-27° 22'	149° 27'	EcoRI – BglII	1,530,791
16	<i>C. glaucophylla</i>	Pilbara	CglHR1	-24° 57'	118° 51'	EcoRI – BglII	2,336,438
14	<i>C. glaucophylla</i>	Central Australia	CglCA1	-23° 03'	132° 39'	EcoRI – BglII	1,255,210
19	<i>C. glaucophylla</i>	Southwest	CglWA1	-31° 20'	121° 19'	EcoRI – BglII	1,340,860
23	<i>C. verrucosa</i>	Southwest	CverLK	-34° 54'	119° 07'	EcoRI – BglII	809,162

The total number of cleaned reads generated by a Miseq sequencer (Illumina, San Diego, USA) was 12,725,050 (ranging from min. 614,007 to max. 2,336,438 per sample). A RAD reference for *Callitris columellaris* species complex was constructed by de novo assembling the reads using CLC Genomics Workbench 7.5.1 (CLC bio, Aarhus, Denmark) (parameter used: mismatch cost 3, insertion and deletion cost 2, length fraction 0.5, similarity fraction 0.9), which resulted in 392,320 contigs with N50 length of 163 bp.